5th Australasian Congress on Applied Mechanics, ACAM 2007
10-12 December 2007, Brisbane, Australia

An Analytical Model for a Twisted Beam Piezoelectric Ultrasonic Micromotor

Aisha Qi, James Friend and Leslie Yeo

Micro/Nanophysics Research Laboratory,
Monash University, Clayton, VIC 3800, Australia

Abstract: An equivalent circuit, known as a Mason model, is proposed to characterize a novel ultrasonic motor in this study. This motor, which consists of a non-circular cross-section twisted beam and a piezoelectric element, generates coupled longitudinal-torsional vibration upon application of an electric field. The model predictions and experimental data are in good agreement. For example, under the condition of having input voltage of 100 Vp−p, and driving frequency of 352.8 kHz, the model predicts a longitudinal velocity of 0.7 m/s compared to the experimental results of 0.65-0.75 m/s. The assumption is that the torsional velocity and longitudinal velocity are in a linear relationship; a proportionality coefficient K=0.259±0.012 is obtained through the experimental data by empirically fitting.

Keywords: equivalent circuit, ultrasonic motor, Mason model, piezoelectric, twisted beam.

1 Introduction

A motor of which the driving force is directly transmitted from the stator to the rotor by friction has its mechanical vibration is driven at frequencies above 20 kHz and is so called ultrasonic motor. Compared to the conventional magnetic D.C. motors, the ultrasonic motors have more widespread application in military, medical and other consumer products due to their unique characteristics, such as smaller volume, larger output torque, lower energy consumption, and quicker and silent response [1-5].

Based on the nature of the driving oscillation, ultrasonic motors can be categorized into two types, the motors driven by travelling waves such as the Wedge-Type motor by Sashida [1], and the motors driven by standing waves. The latter can be further divided due on their vibration modes, such as, sole longitudinal, torsional vibration or other compound modes, such as longitudinal-torsional vibration or longitudinal-bending vibration [2]. Ultrasonic motors that driven under the longitudinal-torsional vibration mode can be further subdivided into two types based on how the vibration is excited. The first type uses the radially poled PZT and the longitudinal poled PZT together to generate both longitudinal and torsional vibration. One example is a hybrid transducer-type ultrasonic motor [3, 4]. However, this type of motor is costly because of the usage of the expensive radially poled PZT. The other type avoids using the radially poled PZT and generates the coupled longitudinal-torsional vibration by converting the longitudinal vibration into torsional vibration with vibration transducers, an example is an ultrasonic motor using a one-dimensional longitudinal-torsional vibration converter with diagonal slits [7]. However, this motor is too large (15 mm to 50 mm in diameter) to be employed in microdevices.

To avoid using the expensive radially poled PZT and to allow micron manufacture, Friend et al. [6] proposed a novel ultrasonic motor that utilizes a non-circular cross-section twisted beam to generate coupled longitudinal-torsional vibration from only one piece of longitudinally poled PZT as shown in Fig. 1(a). The twisted beam is driven by the longitudinal expanding PZT and generates coupled longitudinal-torsional vibration by its specific characteristics: when being stretched, it tends to be untwisted and converts the longitudinal motion to the coupling longitudinal-torsional vibration. [6]. However, the dynamics of this novel motor needs to be identified in order to establish a model for the control of this motor.

In this study, by employing of the Mason equivalent circuit [9, 10], which is a useful method for analyzing longitudinal and the thickness expanding ceramics or other bulk materials, we success to describe the dynamics of this micromotor. As the twisted beam's complex geometries, the exact determination is complicated, so, we assume the beam to be straight to simplify the analysis and to obtain straightforward correspondence with the Mason model for bulk longitudinal expansion.

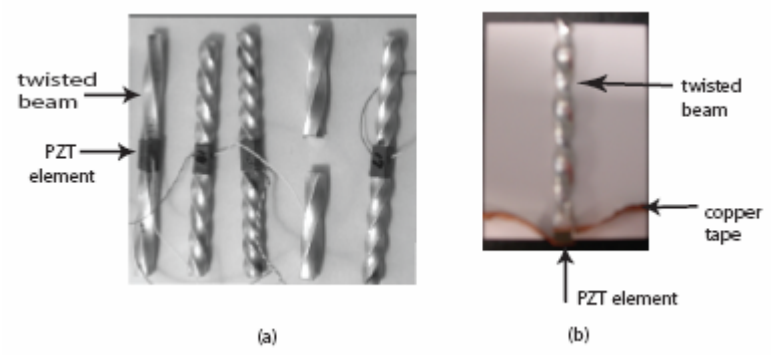

Fig. 1 Illustration of (a) the micromotor proposed by Friend et al. [6], and, (b) the simplified motor used in the current experiment.

2 EQUIVALENT CIRCUIT MODEL

2.1 Model without damping

Fig. 2(a) shows the Mason model [8-10] for the PZT element. Since the electrodes are very thin, their effects can be effectively ignored and only the effect from the PZT elements will be concerned in this equivalent circuit. The parameters used in this figure and in the following analysis are described in Table 1.

Table 1. MODEL PARAMETERS

	Definition	Value		Definition	Value
C_0	static capacitance	ε^s S/d	D	width of the piezoelectric material	0.0035 m
ε_0	relative permittivity constant in vacuum	8.854×10^{-12} F/m	L	length of the piezoelectric material	0.0035 m
ε^s	relative permittivity	$700\varepsilon_0$ F/m	S	cross-sectional area of the piezoelectric material	0.0035^2 m^2
Zp	characteristic impedance of PZT	$Zp = (ckS)/\omega$	Zb	characteristic impedance of the beam	$Zb = (S_b c_b k_b)/\omega$
h	-	e/ε^s	k_b	coupling coefficient	$k=\omega/(c_b/\rho_b)^{1/2}$
e_{33}	piezoelectric stress constant	23	c_b	elastic constant of the beam	7.2×10^{10} N/m^2
k	piezoelectric coupling coefficient	$k=\omega/(c/\rho)^{1/2}$	ρ_b	density of the beam	2.7×10^3 kg/m^3
C	elastic constant, or Young's modulus	6.6×10^{10} N/m^2	S_b	cross-sectional area of the beam	0.003×0.004 m^2
ρ	density of the piezoelectric material	7.72×10^3 kg/m^3	d_b	length of the beam	0.06m

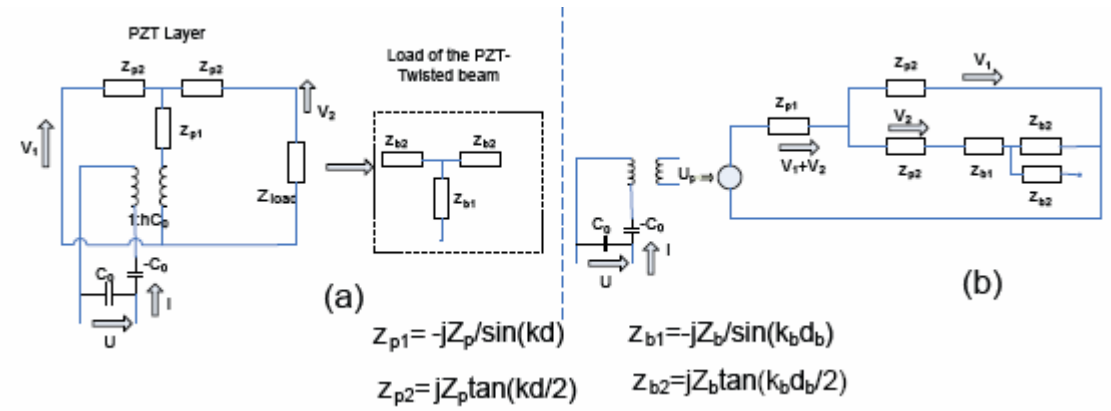

Fig.2 Mason model for the motor without damping

When electrical power is applied to the PZT element, the input voltage is transformed by an electromechanical transformer hC_0 to an equivalent "mechanical voltage", which is the driving source generated in the PZT element. The wave from this source propagates in two directions to generate longitudinal vibration, so we have

$$z_{p1} = \frac{-jZ_p}{\sin(kd)} = \frac{1}{j\omega C}, \tag{1}$$

and

$$z_{p2} = jZ_p \tan(kd/2) = j\omega L. \tag{2}$$

Where z_{p1}, and z_{p2} form a triangular impedance group to describe the PZT element. ω is the driving frequency, which is also the PZT's resonant frequency; z_{p1} is the impedance of a capacitor which represents its stiffness (1/C); and z_{p2} is the impedance of an inductor that stands for the inertia of an effective mass L.

Fig. 2(b) shows the Mason model [8-10] for the motor system. In the same way, a triangular impedance group is employed to characterize the dynamics of the twisted beam that is attached to one of the sides of the PZT element.

By using Kirchhoff's Law, the total current of the circuit can be calculated by,

$$v_1 + v_2 = U_p / z_t, \tag{3}$$

where

$$U_p = hC_0\left(U - \frac{hC_0(v_1+v_2)}{-j\omega C_0}\right) = hC_0\left(U + \frac{hC_0(v_1+v_2)}{j\omega C_0}\right) \tag{4}$$

The equivalent total impedance can be calculated from

$$z_t = \frac{-jZ_p}{\sin(kd)} + \frac{1}{[jZ_p \tan(kd/2)]^{-1} + [z_b + jZ_p \tan(kd/2)]^{-1}}, \tag{5}$$

and

$$z_b = \frac{-jZp}{\sin(k_b d_b)} + jZp \tan(k_b d_b/2). \tag{6}$$

The current v_2, which also represents the longitudinal velocity in the micromotor, flows out of the branch circuits; its value can be calculated from

$$v_2 = \frac{v_1 + v_2}{2jZ \tan(kd/2) + z_b} jZ \tan(kd/2). \tag{7}$$

2.2 Model with damping

The model described above does not take damping effects into account. If damping is present, the velocity will have a finite value at each resonant frequency with a fixed voltage, and the longitudinal velocity can approach a maximum value at the fundamental resonant frequency. Fig. 3 shows the model with damping effect, where the resistor with resistance R allows for the inclusion of damping effects.

The value of the damping R can be calculated by using

$$Q = (L/C)^{1/2} / R, \tag{8}$$

where *L* and *C* can be calculated from equations (1) and (2). *Q* is the quality factor, given by

$$Q = 0.5\left(\frac{f_r + f_a}{f_a - f_r}\right), \quad (9)$$

where f_r is the resonant frequency and f_a is the anti-resonant frequency [11, 16].

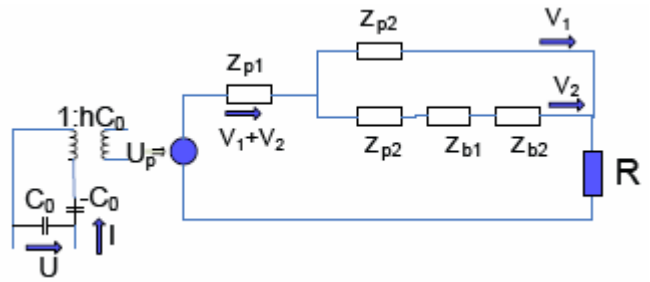

Fig. 3 Model in the presence of damping effects, as accounted for by the inclusion of the resistor R.

2.4 The Assumption about the linear relationship between the torsional velocity and the longitudinal velocity

With the assumption of the torsional vibration has a linear relationship with the longitudinal vibration of the beam:

$$v_{tor} = Kv_{axial}, \quad (10)$$

where v_{tor} is the torsional velocity at the top of the beam and v_{axial} is the longitudinal velocity.

The proportionality coefficient K can either be a constant or either spatially in the longitudinal direction x, or temporally in time t. When K is only a function of x, it is possible to write

$$K(x) = \sum_{j=0}^{m} a_j x^j = a_m x^m + a_{m-1}x^{m-1} + ... + a_1 x^1 + a_0, \quad (11)$$

where a_j $(j = 0, 1, 2, ..., m)$ are unspecified coefficients. With the small displacement $x \ll 1$, hence $K \sim a_0$, suggesting that K does not depend on x to leading order. If K is only a function of t,

$$K(x) = \sum_{k=0}^{n} b_k t^k = b_n t^n + b_{n-1}t^{n-1} + ... + b_1 t^1 + b_0, \quad (12)$$

where b_k $(k = 0, 1, 2, ..., n)$ are unspecified coefficients. For the typical frequencies applied at the order of 10^5 ~10^6 Hz, t « 1 and hence K ~ b_0, again the K is approximately a constant. When K is both spatially and temporally dependent, we have

$$K(x,t) = \sum_{j=0}^{m}(a_j k^j \cdot \sum_{k=0}^{n} b_k t^k). \quad (13)$$

Thus, $K \sim a_0 + b_0$, for $x \ll 1$ and $t \ll 1$, and again is constant to leading order.

From above, it is possible to assume that the torsional velocity is proportional to the longitudinal velocity because of the small displacement and high frequency limit. The value of K is expected to be varied with the shape of the twisted beam. This simplifying assumption will be verified experimentally in the next section.

3 EXPERIMENTS

3.1 Experimental setup

A rigid aluminium twisted beam (47.50 mm in length and 2.75 mm× 3.95 mm in cross-section), was attached to one side of a thickness-expanding PZT element (3.5 mm×3.5 mm×3.5 mm in dimension).

The experiment setup is shown in Fig. 4. A Laser Doppler Vibrometer (Graphtec LDV) was used to measure the torsional (Fig. 4a) and longitudinal (Fig. 4b) velocities of the twisted beam. A thin rigid square aluminium oxide plate attached on top of the twisted beam was used to measure the in-plane torsional velocity, The plate generated an in-plane variation in the horizontal displacement AA' as shown in Fig. 4(a) when it rotated with the same angular velocity of the beam. Since AA' ~ (10^{-5} ~ 10^{-6}) m was much smaller than the radius of this ceramic (6.35 mm), it followed that AA' ≈ AB, where AB could be determined directly from the LDV measurement. Three different plates of the same thickness (1 mm) but with different radii (6.35 mm, 10.55 mm and 12.75 mm) were used in this experiment.

3.2 Linear relationship between torsional and longitudinal velocities

The torsional velocity against the longitudinal velocity of the motor is given in Fig. 5. As can be seen, the relationship between the two velocities is approximately linear. The proportional constant *K* which describes the linear relationship between the torsional and longitudinal velocities was calculated and was found a value of "0.259±0.012". Theoretically, the curves in Fig. 5 are expected to shift downwards slightly with increasing plate radii, but the shift is too small to be seen in the results. This could occurred because the differences between the plate radii are too small to create an observable shift.

3.3. Maximum longitudinal velocity at resonant frequencies

The longitudinal velocities at the motor's resonant frequencies are illustrated in Fig. 6. The solid curves were obtained from the model while the dotted lines were obtained from the experimental results. Fig. 6(a) shows that the longitudinal velocity of the twisted beam can approach infinite values at the resonant frequency in the absence of damping, whereas Fig. 6(b) shows a finite cut-off at each resonant frequency and a maximum of 0.7 m/s when the damping is present.

4. Conclusions

In this paper, the Mason model has been employed to develop an equivalent circuit model to describe the dynamics of a novel twisted beam piezoelectric micromotor. The experimental results and the model estimation show a good agreement. This model can be used to estimate the motor's longitudinal velocity and torsional velocity, as well as its output longitudinal force and torque, at a given specified input voltage. The results of this model can be used to establish a scheme for the control of the twisted beam piezoelectric micromotor.

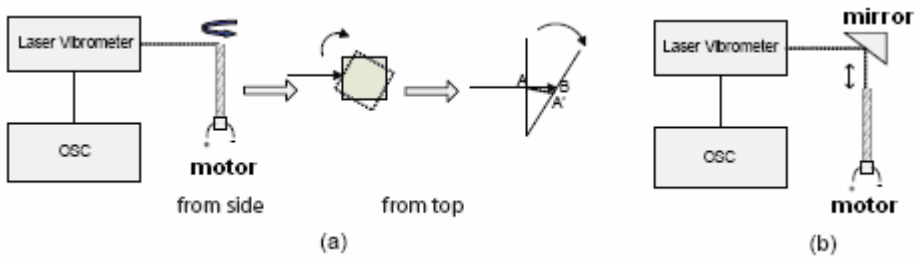

Fig. 4 Experimental setup for measuring (a) the torsional vibration, and (b) the longitudinal vibration of the twisted beam.

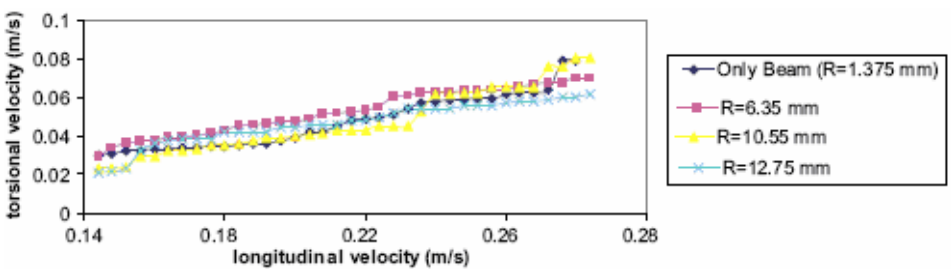

Fig.5 Comparison between the longitudinal velocity and the torsional velocity: the curves illustrate the proportional relationship between the longitudinal and torsional velocities.

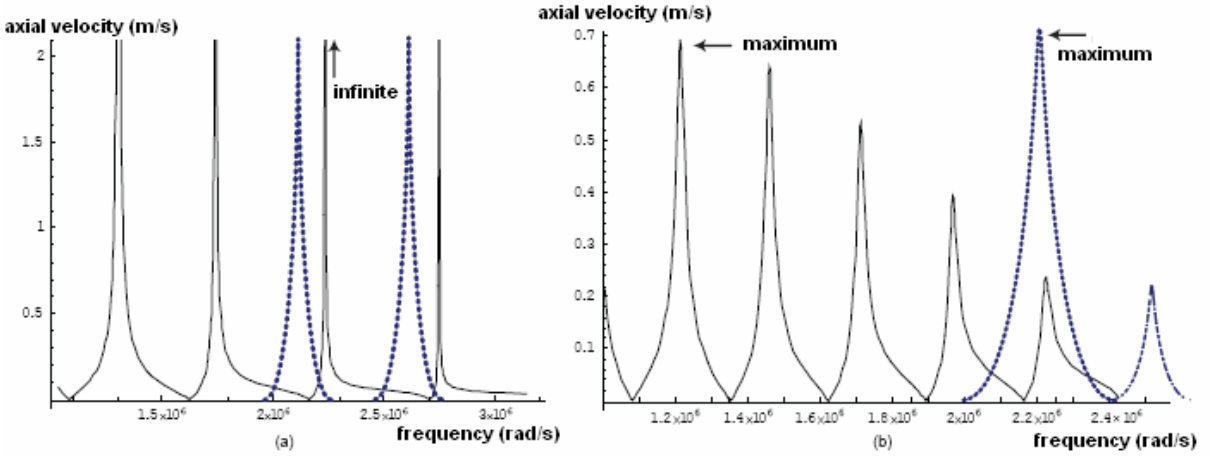

Fig.6 Maximum longitudinal velocity at the resonant frequencies. (a) No damping. (b) Damping.

References

[1] T. Sashida, T. Kenjo, An Introduction to Ultrasonic Motors, Oxford University Press, pp. 5-16, 1993.

[2] S. Lin, "Study on the longitudinal-torsional compound transducer with slanting slots," J. Acoust. Soc. Am, vol. 105, no. 3, pp. 1643-1650, 1999.

[3] K. Nakamura, M. Kurosawa, and S. Ueha, "Characteristics of a hybrid transducer-type ultrasonic motor," IEEE Trans. Ultrason., Ferroelect., Freq. Contr., vol. 38, no. 3, pp. 188-193, 1991.

[4] K. Nakamura, M. Kurosawa, and S. Ueha, "Design of hybrid transducer type ultrasonic motor," IEEE Trans. Ultrason., Ferroelect., Freq. Contr., vol. 40, no. 4, pp. 395-400, 1993.

[5] J. Tsujino, S. Atsuyuki, "Load characteristics of ultrasonic motor with a longitudinal-torsional converter and various nonlinear springs for inducing static pressure," Jap. J. Appl. Phys. Part 1: Regular Papers and Short Notes and Review Papers, vol. 41, no. 5B, pp. 3267-3271, 2002.

[6] J. Friend, K. Nakamura, S. Ueha, "Torsional transducers using asymmetrically twisted bars," ICA, vol. 3, pp. 2251-254, 2004.

[7] K. Nakamura, M. Kurosawa, H. Kurebayashi and S. Ueha, "An estimation of load characteristics of an ultrasonic motor by mearsuring transient response," IEEE Trans. Ultrason., Ferroelect., Freq. Contr., vol. 38, no. 5, pp. 481-485, 1991.

[8] W. P. Mason, Electromechanical Transducers and Wave Filters, second edition, New York, D. Van Nostrand Co., 1948.

[9] D. Royer, E. Dieulesain, Elastic Waves in Solids, Springer, pp. 6-14, 2000.

[10] R. Kriholtz, D. A. Leedom, G. L. Matthaei, "New equivalent circuits for elementary piezoelectric transducers," electron. lett., vol 6, no.13, pp. 398-399, 1970.

[11] IEEE Standard on Piezoelectricity, Inst. Electr. & Electron. Eng., New York, NY, USApp., pp.50-52, 1998.

[12] G. Bal, E. Berkiro˘glu, "A highly effective load adaptive servo drive system for speed control of travelling-wave ultrasonic motor," IEEE Trans. Power Electron., vol. 20, no. 5, pp. 1143-1149, 2005.

[13] S. sherrit, H. D. Wiederic, B. K. Mukherjee and M. sayer, "An accurate equivalent cirvuit for the unloaded piezoelectric vibrator in the thickness mode," J. Phys. D, Appl. Phys. vol. 30, no. 16, pp. 2354-2363, 1997.

[14] M. Onoe and H. Jumonji, "Useful formulas for piezoelectric ceramic resonantors and their application to measurment of parameters," Acoust. Soc. Am. vol. 41, no. 4, pp. 974-980, 1967.

[15] P. Gonnard, "Investigation on dielectric, mechanical and piezoelectric non-linearities in piezoelectrics through a new equivalent crcuit," IEEE Int. Symp. Appl. Ferroelectr., vol. 2, pp. 691-694, 2001.

[16] J. H. Cho, R. F. Richards, D. F. Bahr, C. D. Richards, M. J. Anderson, "Efficiency of energy conversion by piezoelectrics," Appl. Phys. Lett., vol. 89, no. 10, pp. 104-107, 2006.

[17] J. H. Cho, M. Anderson, R. Richards, D. Bahr and C. Richards, "Optimization of electromechanical coupling for a thin-film PZT membrane:I. Modeling," J. Micromech. Microeng., vol. 15, no. 10, pp. 1797-1803, 2005.

[18] C. D. Richards, M. J. Anderson, D. F. Bahr and R. F. Richards, "Efficiency of energy conversion for devices containing a piezoelectric component," J. Micromech. Microeng., vol. 14, no. 5, pp. 717-721, 2004.